Optical storage with electromagnetically induced transparency in a dense cold atomic ensemble

Shanchao Zhang, Shuyu Zhou, M. M. T. Loy, G. K. L. Wong, and Shengwang Du*

Department of Physics, The Hong Kong University of Science and Technology, Clear Water Bay, Kowloon, Hong Kong, China
**Corresponding author: dusw@ust.hk*

Received August 22, 2011; revised October 18, 2011; accepted October 18, 2011;
posted October 19, 2011 (Doc. ID 153184); published November 23, 2011

We experimentally investigate optical storage with electromagnetically induced transparency in a dense cold ^{85}Rb atomic ensemble. By varying the optical depth (OD) from 0 to 140, we observe that the optimal storage efficiency has a saturation value of 50% as OD > 50. Our result is consistent with that obtained from hot vapor cell experiments. © 2011 Optical Society of America

OCIS codes: 210.4680, 020.1670.

Optical storage is a key step toward the realization of long-distance all-optical communication networks [1]. Such a process requires coherently mapping photonic states into and out of an optically controlled memory on demand. In both classical and quantum communication networks, the storage efficiency, defined as the ratio of retrieved pulse energy to that of the input, plays an important role in practical applications. In the past decade, much effort has been made in developing atomic quantum memories based on light–atom interactions, such as electromagnetically induced transparency (EIT [2,3], including the off-resonance Raman scheme) and photon echoes [4–6]. So far, a high storage efficiency of more than 80% has been achieved only by the photon-echo method [7]. However, experimental demonstrations of photon-echo-based memory have all been limited to classical light pulses, and its access to quantum state storage remains a challenge. Meanwhile, this method requires additional control of reversible inhomogeneous broadening or an atomic frequency gradient, which is difficult to achieve optically.

In this Letter, we focus our work on the EIT-based optical memory that has been proved to be compatible with quantum state operations of single-photon wave packets [8–10] and squeezed states [11,12]. Since the first demonstrations in 2001 [13,14], EIT storage has been studied in both hot atomic vapor cells [15–17] and cold atoms [18–21]. However, the reported experimental demonstration always has a very low storage efficiency that prevents it from practical applications. To increase the storage efficiency, a high optical depth (OD) is commonly believed to be necessary. Theory predicts that the storage efficiency increases as we increase atomic OD and it approaches to unity at OD > 100 [22]. However, the experimental study in hot atomic vapor cells shows that the storage efficiency is limited by 45%, which is inconsistent with the theoretical prediction [15,16]. Further systematic studies suggest that a four-wave mixing (FWM) nonlinear process may contribute to the loss of the storage efficiency [17]. On the other hand, there is no systematic experimental study with cold atoms due to the difficulty in obtaining high OD. In this work, we report our experimental investigation of optical storage with EIT in a dense cold atomic ensemble whose OD can be varied from 0 up to 140. Similar to that in a hot atomic vapor cell, we find that the optimal storage efficiency has a saturation value of 50% at high OD. Our result, representing the best EIT storage efficiency reported in cold atoms, to the best of our knowledge, provides a reference to understand the loss of EIT memory for future improvement.

The EIT three-level Λ configuration and experiment setup are shown in Fig. 1. We work with a two-dimensional ^{85}Rb magneto-optical trap (MOT) with a longitudinal length $L = 1.7$ cm and a temperature of 100 μK. A weak probe beam, ω_p, on resonance with the transition $|1\rangle \leftrightarrow |3\rangle$, is modulated by an fiber-based amplitude electro-optical modulator (EOM, 10 GHz, EOspace), and passes through the cold atoms along the longitudinal axis. A stronger coupling laser beam, ω_c, on resonance with the $|2\rangle \leftrightarrow |3\rangle$ transition, is collinearly aligned with a small angle of 3° with respect to the probe beam. Both the probe and coupling lasers have the same circular polarization (σ^+) for optimizing the EIT effect with degenerate Zeeman substates. The probe beam is focused on the center of the atomic cloud with a $1/e^2$ diameter of 245 μm. The coupling beam has a $1/e^2$ diameter of 1.46 mm, and its intensity is controlled by a 181 MHz acoustic-optical modulator (Brimrose). To further suppress the scattering light from the coupling beam, we couple the probe beam into a single-mode fiber (SMF) before it is detected by a photomultiplier tube (PMT, Hamamatsu, H6780-20, with 0.78 ns rise time). The EOM is driven by a fast waveform function generator (Tektronix, AFG3252, with 3 ns rise time). The experiment runs periodically. In each cycle, after the MOT trapping time of 4.5 ms, the atoms are prepared at the

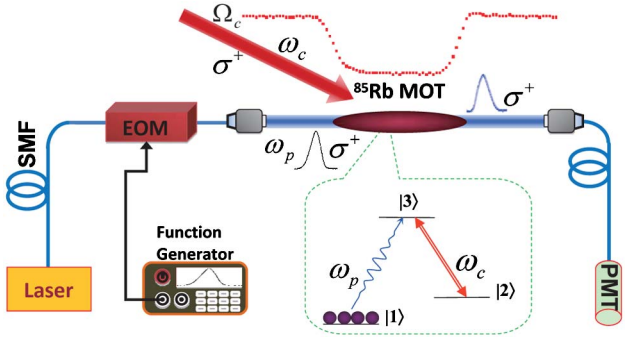

Fig. 1. (Color online) Schematics of the experiment setup. The ^{85}Rb energy levels are chosen as $|1\rangle = |5S_{1/2}, F = 2\rangle$, $|2\rangle = |5S_{1/2}, F = 3\rangle$, and $|3\rangle = |5P_{1/2}, F = 3\rangle$.

ground state $|1\rangle$. During the 0.5 ms measurement window, all the MOT trapping and repump lasers are switched off but the magnetic field remains on all the time. This two-dimensional MOT configuration allows us to vary the OD in a large parameter range from 0 up to 140. The OD value is determined by using a least-squares fit from the probe absorption spectrum (without EIT) with a frequency detuning range from −40 to 40 MHz.

We first measure the EIT spectrum by scanning the probe frequency in a steady-state condition. At OD = 140 and coupling laser power of 2.4 mW, the measured probe transmission spectrum is shown in Fig. 2(a). We obtain the coupling laser Rabi frequency $\Omega_c = 5.6\gamma_{13}$ by best fitting the EIT spectrum (the red solid curve), which agrees well with the calculated value from the measured laser power and beam diameter. Here $\gamma_{13} = 2\pi \times 3$ MHz is the electric dipole relaxation rate between $|1\rangle$ and $|3\rangle$, obtained from the probe absorption natural (angular frequency) linewidth $\Gamma = 2\pi \times 6$ MHz (without presence of the coupling laser) using the relation $\gamma_{13} = \Gamma/2$. We estimate the ground-state dephasing rate between $|1\rangle$ and $|2\rangle$ as $\gamma_{12} = 0.01\gamma_{13}$, which fits best to the EIT measurement. The coupling laser creates a narrow transparency window with a width of 3 MHz. Under the same condition, we measure the group delay by sending a long Gaussian probe pulse with 1 μs full width at half-maximum (FWHM). As illustrated in Fig. 2(b), we observe a pulse peak delay of 360 ns and the transmitted pulse energy is about 73% of that of input.

We now start to perform optical storage. The dynamical EIT mechanism is described as the following. When a probe pulse enters the medium, it slows down and is compressed spatially. After the probe pulse is compressed inside the medium, we switch off the coupling laser and convert the probe optical field into a long-lived atomic spin wave [3]—this is called the writing process. After a controllable time delay in the reading process, we switch on the coupling beam (reversibly) and convert the atomic spin wave back to the probe pulse. It has been both theoretically and experimentally shown that the amplitude–phase information of the probe pulse is coherently preserved [19,22]. The storage efficiency is obtained as $\eta = \int |E_{\rm out}(t)|^2 {\rm d}t / (\int |E_{\rm in}(t)|^2 {\rm d}t)$, where $E_{\rm in}(t)$ and $E_{\rm out}(t)$ are the input and output probe fields. Because of the finite atomic coherence time $1/(2\gamma_{12})$, the storage efficiency drops as the storage time increases. Here we define the storage time as the duration when the coupling laser is switched off completely. In a practical application, the merit value is the product of the storage efficiency and the storage time. In the following experiment and discussion, we optimize the EIT storage efficiency at a two pulse-length (i.e., 2 bit) storage time.

We vary OD from 0 up to 140. At each OD, we optimize the storage efficiency at a 2-bit storage time following the optimization process described in [15]. The coupling laser is switched off and on with a fall and rise time of 50 ns. With a given coupling laser power, the probe pulse shape is optimized for achieving maximum storage efficiency. Figure 3(a) illustrates an optimized storage process at OD = 60 and $\Omega_c = 11.5\gamma_{13}$. The nearly Gaussian-shaped input probe pulse has a FWHM length of 50 ns. With the coupling laser run in a cw mode, the peak of the probe pulse is delayed by 35 ns. In the storage experiment, the coupling laser is switched off completely at time $t =$ 0 ns and switched on back at $t = 100$ ns. The retrieved probe pulse with a storage efficiency of 51% is shown as the blue open circle points whose peak is delayed by 200 ns compared to the input pulse. The retrieved pulse at $t < 0$ is the leakage field that has not been converted into an atomic spin wave. Figure 3(b) shows the optimal storage efficiency η_m as a function of OD with the same coupling Rabi frequency, and the red solid curve is fitted with an exponential growth function. It is clear that η_m is limited by 50% after the OD reaches more than 50. Because of the nonzero dephasing rate γ_{12}, the storage efficiency is also a function of coupling laser intensity. We confirm this by reducing the coupling power by a factor of 1/2; the

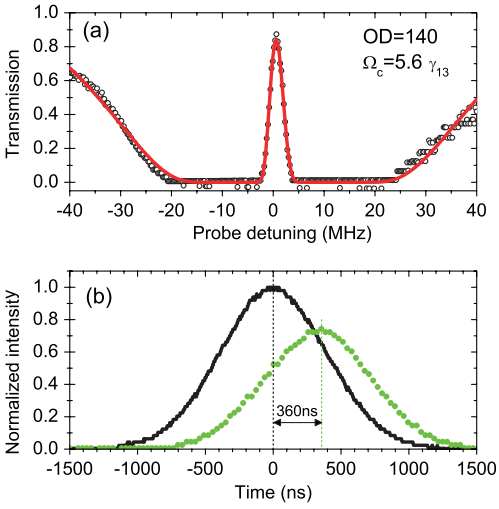

Fig. 2. (Color online) (a) Probe laser EIT transmission profile. (b) Slow light effect of a Gaussian pulse propagation.

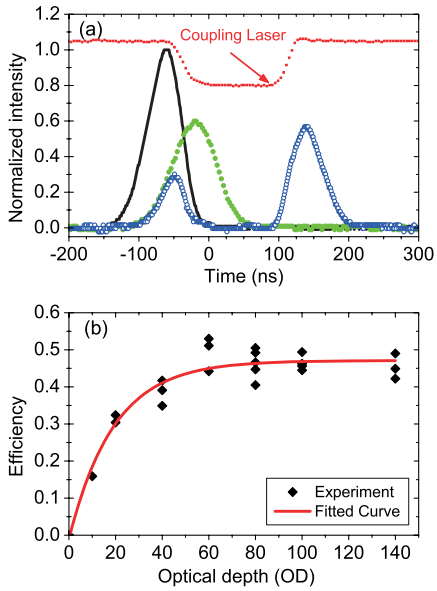

Fig. 3. (Color online) (a) EIT optical storage measurement at OD = 60. The black solid curve is the input probe pulse. The green dotted curve is the delayed probe pulse as the coupling laser is in cw mode. The retrieval pulse (blue open circles) has a storage efficiency of 51%. (b) Optimal storage efficiency as a function of OD. In both (a) and (b), the coupling Rabi frequency is $\Omega_c = 11.5\gamma_{13}$.

saturation storage efficiency drops to 41%. On the other hand, as we increase the coupling power by a factor of 2, we see no increase of the storage efficiency. Therefore, 50% represents the best storage efficiency we can achieve in this system.

In conclusion, we have studied EIT-based optical storage in cold atomic ensembles with OD ranging from 0 to 140. We found that the optimal storage efficiency reaches the saturation value of 50% as OD > 50. This result is consistent with the previous studies in hot rubidium vapor cells, which suggests that the FWM nonlinear process degrades the EIT storage coherence and efficiency [15–17]. In such a FWM process, the on-resonance coupling laser, while rendering the EIT effect for the probe laser, also acts as an off-resonance pump field in the transition $|1\rangle \rightarrow |3\rangle$. In our configuration, it is detuned by 3 GHz due to the hyperfine splitting between the two ground levels. The generated Stokes field following this pump process, together with the coupling and probe fields, closes the FWM loop. As shown by the Novikova group [17], such a FWM process significantly reduces the EIT storage efficiency at a high OD. Our recent experiment using this process to produce hyperentangled paired photons demonstrated that this FWM process always naturally occurs in the EIT system [23].

The work was supported by the Hong Kong Research Grants Council (Project No. 600710, DAG_S09/10.SC06, and DAG08/09.SC02). The authors also acknowledge valuable suggestions from the reviewers.

References

1. L. M. Duan, M. D. Lukin, J. I. Cirac, and P. Zoller, Nature **414**, 413 (2001).
2. S. E. Harris, Phys. Today **50**, 36 (1997).
3. M. Fleischhauer, A. Imamoglu, and J. P. Marangos, Rev. Mod. Phys. **77**, 633 (2005).
4. T. W. Mossberg, Opt. Lett. **7**, 77 (1982).
5. A. L. Alexander, J. J. Longdell, M. J. Sellars, and N. B. Manson, Phys. Rev. Lett. **96**, 043602 (2006).
6. M. Hösseini, B. M. Sparkes, G. Hétet, J. J. Longdell, P. K. Lam, and B. C. Buchler, Nature **461**, 241 (2009).
7. M. Hösseini, B. M. Sparkes, G. Campbell, P. K. Lam, and B. C. Buchler, Nat. Commun. **2**, 174 (2011).
8. T. Chanelière, D. N. Matsukevich, S. D. Jenkins, S.-Y. Lan, T. A. B. Kennedy, and A. Kuzmich, Nature **438**, 833 (2005).
9. M. D. Eisaman, A. André, F. Massou, M. Fleischhauer, A. S. Zibrov, and M. D. Lukin, Nature **438**, 837 (2005).
10. K. S. Choi, H. Deng, J. Laurat, and H. J. Kimble, Nature **452**, 67 (2008).
11. K. Honda, D. Akamatsu, M. Arikawa, Y. Yokoi, K. Akiba, S. Nagatsuka, T. Tanimura, A. Furusawa, and M. Kozuma, Phys. Rev. Lett. **100**, 093601 (2008).
12. J. Appel, E. Figueroa, D. Korystove, M. Lobino, and A. I. Lvovsky, Phys. Rev. Lett. **100**, 093602 (2008).
13. C. Liu, Z. Dutton, C. H. Behroozi, and L. V. Hau, Nature **409**, 490 (2001).
14. D. F. Phillips, A. Fleischhauer, A. Mair, R. L. Walsworth, and M. D. Lukin, Phys. Rev. Lett. **86**, 783 (2001).
15. I. Novikova, A. V. Gorshkov, D. F. Phillips, A. S. Sørensen, M. D. Lukin, and R. L. Walsworth, Phys. Rev. Lett. **98**, 243602 (2007).
16. N. B. Phillips, A. V. Gorshkov, and I. Novikova, Phys. Rev. A **78**, 023801 (2008).
17. N. B. Phillips, A. V. Gorshkov, and I. Novikova, Phys. Rev. A **83**, 063823 (2011).
18. Y.-F. Chen, S.-H. Wang, C.-Y. Wang, and I. A. Yu, Phys. Rev. A **72**, 053803 (2005).
19. Y. F. Chen, Y. C. Liu, Z. H. Tsai, S. H. Wang, and I. A. Yu, Phys. Rev. A **72**, 033812 (2005).
20. Y.-F. Chen, P.-C. Kuan, S.-H. Wang, C.-Y. Wang, and I. A. Yu, Opt. Lett. **31**, 3511 (2006).
21. Y. W. Lin, H. C. Chou, P. P. Dwivedi, Y. C. Chen, and I. A. Yu, Opt. Express **16**, 3753 (2008).
22. A. V. Gorshkov, A. André, M. Fleischhauer, A. S. Sørensen, and M. D. Lukin, Phys. Rev. Lett. **98**, 123601 (2007).
23. H. Yan, S. Zhang, J. F. Chen, M. M. T. Loy, G. K. L. Wong, and S. Du, Phys. Rev. Lett. **106**, 033601 (2011).